



# Patient-specific 3D printed model of biliary ducts with congenital cyst

Amee Allan<sup>1</sup>, Catherine Kealley<sup>1</sup>, Andrew Squelch<sup>2,3</sup>, Yin How Wong<sup>4</sup>, Chai Hong Yeong<sup>4</sup>, Zhonghua Sun<sup>1</sup>

<sup>1</sup>Discipline of Medical Radiation Sciences, School of Molecular and Life Sciences, Curtin University, Perth, Western Australia, Australia; <sup>2</sup>Discipline of Exploration Geophysics, Western Australian School of Mines, Minerals, Energy and Chemical Engineering, Curtin University, Perth, Western Australia, Australia; <sup>3</sup>Computational Image Analysis Group, Curtin Institute for Computation, Curtin University, Perth, Western Australia, Australia; <sup>4</sup>School of Medicine, Faculty of Health and Medical Sciences, Taylor's University, Subang Jaya, Malaysia

*Correspondence to:* Prof. Zhonghua Sun, Discipline of Medical Radiation Sciences, School of Molecular and Life Sciences, Curtin University, GPO Box U1987, Perth, Western Australia 6845, Australia. Email: z.sun@curtin.edu.au.

**Background:** 3D printing has shown great promise in medical applications, with increasing reports in liver diseases. However, research on 3D printing in biliary disease is limited with lack of studies on validation of model accuracy. In this study, we presented our experience of creating a realistic 3D printed model of biliary ducts with congenital cyst. Measurements of anatomical landmarks were compared at different stages of model generation to determine dimensional accuracy.

**Methods:** Contrast-enhanced computed tomography (CT) images of a patient diagnosed with congenital cyst in the common bile duct with dilated hepatic ducts were used to create the 3D printed model. The 3D printed model was scanned on a 64-slice CT scanner using the similar abdominal CT protocol. Measurements of anatomical structures including common hepatic duct (CHD), right hepatic duct (RHD), left hepatic duct (LHD) and the cyst at left to right and anterior to posterior dimensions were performed and compared between original CT images, the standard tessellation language (STL) image and CT images of the 3D model.

**Results:** The 3D printing model was successfully generated with replication of biliary ducts and cyst. Significant differences in measurements of these landmarks were found between the STL and the original CT images, and the CT images of the 3D printed model and the original CT images ( $P < 0.05$ ). Measurements of the RHD and LHD diameters from the original CT images were significantly larger than those from the CT images of 3D model or STL file ( $P < 0.05$ ), while measurements of the CHD diameters were significantly smaller than those of the other two datasets ( $P < 0.05$ ). No significant differences were reached in measurements of the CHD, RHD, LHD and the biliary cyst between CT images of the 3D printed model and STL file ( $P = 0.08-0.98$ ).

**Conclusions:** This study shows our experience in producing a realistic 3D printed model of biliary ducts and biliary cyst. The model was found to replicate anatomical structures and cyst with high accuracy between the STL file and the CT images of the 3D model. Large discrepancy in dimensional measurements was noted between the original CT and STL file images, and the original CT and CT images of the 3D model, highlighting the necessity of further research with inclusion of more cases of biliary disease to validate accuracy of 3D printed biliary models.

**Keywords:** Biliary disease; cyst; dimensional measurement; three-dimensional (3D) printing; STL file; computed tomography (CT)

Submitted Nov 10, 2018. Accepted for publication Dec 03, 2018.

doi: 10.21037/qims.2018.12.01

**View this article at:** <http://dx.doi.org/10.21037/qims.2018.12.01>

## Introduction

Three-dimensional (3D) printing has been increasingly used in medical applications with creation of accurate patient-specific 3D printed models using medical imaging data (1-4). 3D printed physical models have been shown to improve our understanding of complex anatomy and pathology, assist clinical decision making by serving as a valuable tool for preoperative planning, simulation and education, as well as develop optimal scanning protocols for radiation dose reduction (5-10). A high degree of accuracy of 3D printed models is of paramount importance to assist physicians in developing personalized medicine for patient's treatment options, thus minimizing risks and complications associated with surgical procedures and improving patient outcomes (11). Applications of 3D printed models are mainly dominated by orthopedics and maxillofacial surgery with increasing roles in cardiovascular disease (12-19), however, its use in hepatobiliary disease is limited.

3D printed liver models have been confirmed to overcome limitations of traditional computed tomography (CT) or magnetic resonance imaging (MRI) imaging by providing accurate assessment of complex hepatic anatomy and pathology, and assisting selection of appropriate surgical procedures for hepatic tumors or liver transplantation (16-20). A recent systematic review has analyzed 19 studies of reporting the usefulness of 3D printed liver models in the simulation of liver surgeries (21). In contrast, research on 3D printing in biliary disease is limited with only a few case reports available in the literature (22-24). Furthermore, model accuracy and clinical value of 3D printed biliary system and disease remains to be determined. Therefore, the purpose of this study was to create a patient-specific 3D printed biliary model with the aim of validating model accuracy by comparing measurements performed at different stages of model generation.

## Methods

### *Selection of a sample case*

A sample case of a patient diagnosed with congenital cyst in the common bile duct with dilated hepatic ducts on CT was selected for generation of the 3D model. Contrast-enhanced CT was performed on a 128-slice dual-source CT scanner (Siemens Definition Flash, Siemens Healthcare, Forchheim, Germany) with the following scanning protocol: detector collimation  $2 \times 64\text{-slice} \times 0.6\text{ mm}$  with gantry rotation of 330 ms, 100 kVp and 282 mAs, a slice thickness of 1.0 mm

with resulting voxel size of  $0.70 \times 0.70 \times 0.70\text{ mm}^3$ .

### *Image post-processing and segmentation*

Original CT images in Digital Imaging and Communications in Medicine (DICOM) format were transferred to a separate workstation with Analyze 12.0 (AnalyzeDirect Inc., Lexana, KS, USA) for post-processing and segmentation. A median filter was first applied to the CT volume data to improve the anatomical boundaries by reducing image noise, followed by the use of manual and semi-automatic segmentation approaches to segment the biliary tree and cyst from the surrounding structures such as soft tissues, bones, and other unwanted structures. Special attention was paid to the anatomical structures of the biliary tract including left hepatic duct (LHD), right hepatic duct (RHD), and common hepatic duct (CHD) which were segmented for inclusion in the final 3D model. A smoothing filter was also applied to the segmented volume data to improve the surface quality of the model. The final dataset was exported into Standard Tessellation Language (STL) format for 3D printing.

The STL file was imported into the Blender ver 2.79b (Stitching Blender Foundation, The Netherlands) open-source software to further edit the digital file (25). During the editing process, some deformities or free-floating objects were removed, with any holes fixed and the model created as hollow. A thickness of 2 mm was added to the external walls of model to ensure the stability of the 3D printed model.

### *3D printing*

The final STL file was printed with an Ultimaker 2 Extended 3D printer from Ultimaker BV (Geldermalsen, Netherlands) using fused filament fabrication (FFF) technology in the material of thermoplastic polyurethane (TPU) 95A. TPU 95A is a semi-flexible material with rubber- and plastic-like properties. The material was used in an attempt to mimic biliary tissue attenuation. *Figure 1* is a flow chart demonstrating the steps of generating the 3D printed model from 2D DICOM data analysis to the generation of STL and 3D printing.

The 3D printed model was scanned on a 64-slice CT (Siemens Somatom Definition AS 64, Siemens Healthcare, Forchheim, Germany) using the scanning protocol of an abdominal CT with the following parameters: 120 kVp and 176 mAs with a slice thickness of 0.75 mm resulting in voxel size of  $0.56 \times 0.56 \times 0.56\text{ mm}^3$ . *Figure 2* shows a series of 2D axial CT images of the 3D printed model with visualization

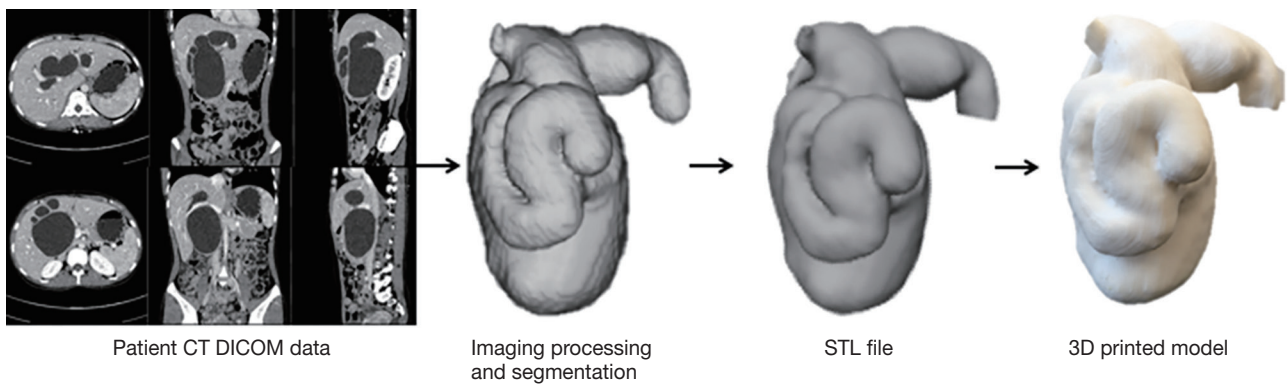


**Figure 1** Flow diagram showing the process of creating 3D printed model from original 2D DICOM images to STL file and 3D printing. DICOM, Digital Imaging and Communications in Medicine; STL, standard tessellation language.

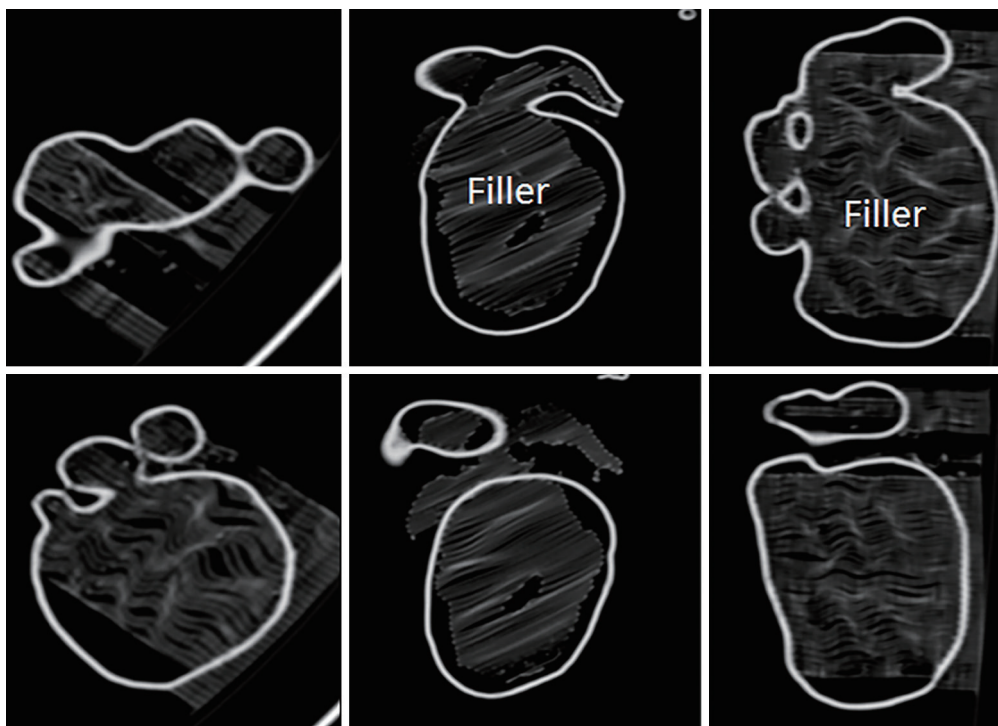


**Figure 2** CT images of the 3D printed biliary model at different anatomical locations showing dilated hepatic ducts and a huge cyst in the common bile duct. A filler material is visible inside the model to prevent it from collapsing during the 3D printing process.

of dilated bile ducts and cyst. A supporting filler is visible inside the model that prevents the model from collapsing during the 3D printing process.

#### *Quantitative assessment of model accuracy*

To ensure the model accuracy, measurements of anatomical

landmarks were performed and compared at three stages of the model production, namely, the original CT images, STL file and CT images of the 3D printed model (*Figure 3*). The internal diameter of four anatomical locations was measured from left to right (LR) and from anterior to posterior (AP) in the following landmarks: CHD, LHD, RHD and biliary cyst. Measurements were repeated three

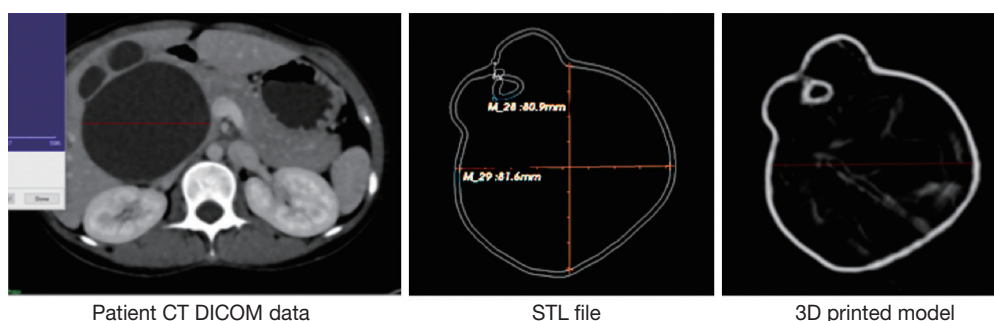


**Figure 3** An example of showing measurement of anatomical landmarks at different stages of model production. Images show measurements of the cyst diameter from left to right dimensions on original CT, STL file and CT of the 3D printed model. CT, computed tomography; STL, standard tessellation language.

times at each location by two independent observers with mean values used as the final ones. An excellent correlation was achieved between the two observers ( $r=0.99$ ,  $P<0.001$ ).

### Statistical analysis

Data were entered into SPSS 24.0 (IBM Corporation, Armonk, NY, USA) for statistical analysis. Continuous variables were presented as mean  $\pm$  standard deviation. A paired sampled t-test was used to determine any significant differences in the measurements between original CT images, CT of the 3D model and STL images. Statistical significance was defined as a P value of less than 0.05.

### Results

The model was successfully printed with excellent demonstration of normal anatomical structures of the biliary duct and the cyst (*Figure 4*). CT attenuation of the 3D model wall was between 40 and 80 Hounsfield Units (HU), which is close to the attenuation of soft tissue on the patient's CT images. The total time taken to generate the 3D printed model was 2.5 hours and the printing process was 72 hours. The cost of printing the model was AUD 50.

*Table 1* shows measurement differences in the anatomical locations between the original CT, STL and CT of the 3D model images. Significant differences were found in measurements between the STL and original CT images, and also between the CT images of the 3D printed model and the original CT images ( $P<0.05$ ). This is especially apparent in measurements of the RHD and LHD diameters with measurements from the original CT images significantly larger than those from the CT images of 3D

model or STL images ( $P<0.05$ ), while measurements of the CHD diameters were significantly smaller than those of the other two datasets ( $P<0.05$ ). No significant differences were noted in measurements of the CHD, RHD, LHD and biliary cyst between CT images of the 3D model and STL file ( $P=0.08-0.98$ ), except for measurements of the RHD at AP dimension in CT images of the 3D model which is significantly smaller than those from the STL file ( $P<0.05$ ).

### Discussion

In this study we present our experience of creating a patient-specific 3D printed model of biliary tree and biliary cyst using CT imaging data. The 3D printed model replicates anatomical structures and pathology with high accuracy between STL and CT images of the 3D model. Significant discrepancy was found in measurements of the anatomical landmarks between the original CT images, the STL images, and the CT images of the 3D model. This indicates the potential errors introduced during image post-processing, segmentation and editing of the data, which need to be addressed in the future image post-processing processes for 3D printing.

Developments of 3D printing technique have led to increased applications in medical field with promising reports of 3D printed models to assist diagnosis, therapeutic planning and treatment of complex diseases. To our knowledge, research on 3D printing in biliary disease is limited with only a few cases reported in the current literature. Takagi *et al.* (26) created a 3D printed model of a patient with intrahepatic cholangiocarcinoma based on a multi-phase contrast-enhanced CT scan. The 3D printed model was found to replicate the macroscopic findings

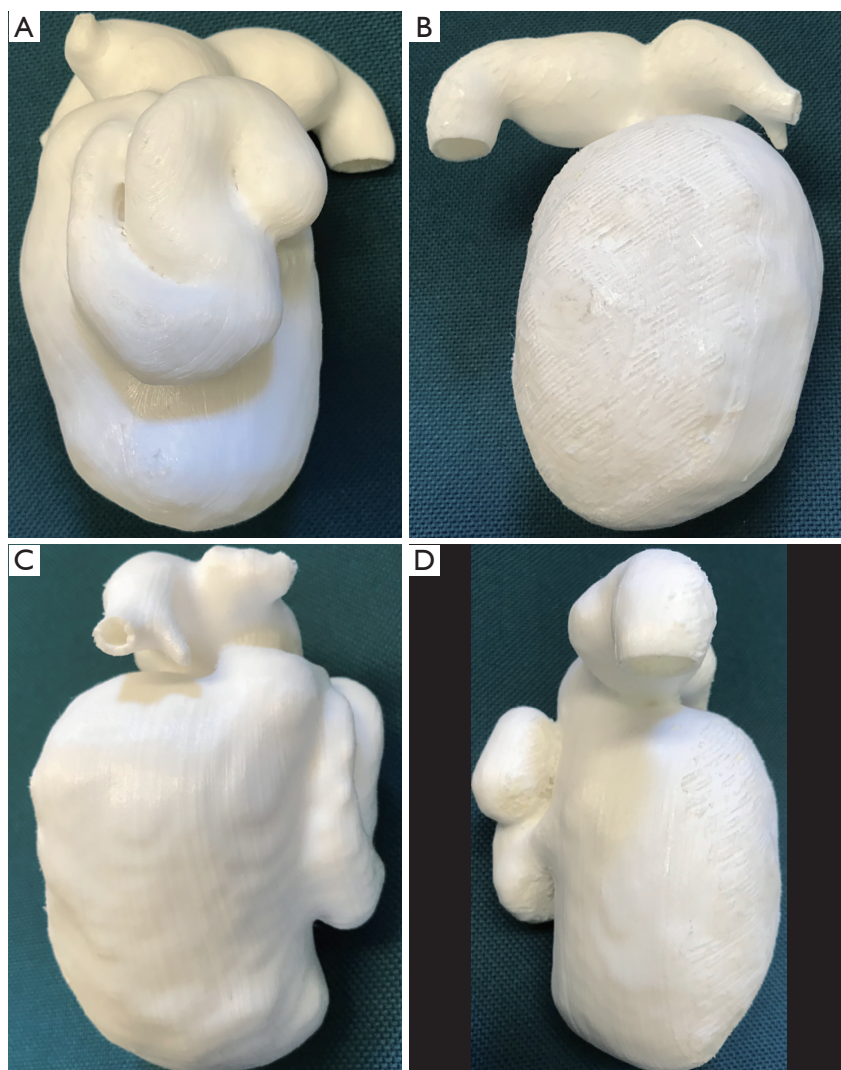


**Figure 4** 3D printed biliary model with different viewing angles. (A-D) Anterior, posterior, left and right views showing the model.

**Table 1** Measurement differences between original CT, STL file and CT of 3D printed model

Landmarks/ comparisons	Differences (%) in measurements by Observer 1/Observer 2					
	STL file compared to original CT		CT of 3D printed model compared to original CT		STL file compared to CT of 3D printed model	
	LR	AP	LR	AP	LR	AP
Common hepatic duct	19.6 [7]/23.8 [4]	6.0 [2]/6.5 [2]	15.2 [3]/18.3 [3]	9.4 [3]/7.6 [2]	3.8 [6]/4.7 [6]	3.8 [7]/1.3 [2]
Right hepatic duct	23.4 [1]/23.2 [2]	19.1 [7]/18.9 [11]	24 [1]/22.9 [2]	28.8 [1]/30.9 [2]	0.80 [3]/0.16 [1]	13.6 [4]/17.3 [8]
Left hepatic duct	22.2 [3]/21.8 [1]	16.9 [5]/13.1 [4]	23.7 [6]/19.0 [6]	21.4 [1]/13.7 [3]	2.0 [3]/3.5 [1]	5.9 [2]/0.7 [2]
Biliary cyst	3.2 [2]/3.8 [3]	2.6 [3]/0.5 [1]	4.4 [3]/3.9 [4]	0.7 [1]/0.2 [1]	1.2 [1]/0.1 [1]	1.8 [1]/0.7 [1]

Numbers in the brackets indicate standard deviation. LR, left to right dimension; AP, anterior to posterior dimension; STL, standard tessellation language; CT, computed tomography.

and demonstrate similar resection when compared to the resected specimen, thus was considered useful for future pre-operative simulations. In another study by Dhir *et al.* (27), a 3D printed prototype of a dilated biliary system was developed and evaluated for the teaching and training of endoscopic ultrasound-guided biliary drainage to endosonographers. The model was deemed suitable for the training of the four important steps of bile duct drainage and it was agreed that it simulated real-life problems. In addition, their study showed that the properties of the polycarbonate material (used to create the prototypes) closely mimicked bile duct walls on radiography and ultrasound. However, none of these studies investigated the model accuracy. This has been addressed in our study as we focused on validating model accuracy by comparing measurements acquired from different stages of model creation. Despite presence of significant discrepancies in measuring some anatomical structures between STL/CT images of the 3D printed model and the original CT images, results of this study provide additional information to the current literature about creating realistic physical models of biliary disease. Future studies with inclusion of more cases are required to confirm dimensional accuracy of the 3D printed biliary models.

A number of studies have demonstrated encouraging results of the usefulness of 3D printed liver models which serve as valuable tools for pre-surgical planning, intra-operative orientation and simulation purposes (16-20). However, a recent systemic review highlights the limited studies involving quantitative assessment of the accuracy of 3D printed liver models (21). Through analysis of five studies reporting quantitative assessment of model accuracy, the review indicates differences between the 3D printed liver model and original CT data of between 0.20% and 20.8%. The results of our study fall within this range, although some differences are close to 31% (*Table 1*) which is larger than those reported in the literature. However, most of the liver models created by other studies were printed at 60–70% of the original size due to high cost, while in our study a 1:1 scale model of the biliary duct and cyst was created to replicate real size of the anatomy and pathology.

There were some limitations in this study. First, only one model was generated with no qualitative assessment on the clinical value of the 3D printed biliary model. More cases with inclusion of different biliary diseases, preferably including malignant tumors are desirable as our study

only included a case with benign cyst. Second, there was a possibility of inconsistency amongst the orientation and location of the measurements of each anatomical landmark between the observers and three datasets which could contribute to some large discrepancy in measurements. Measurements with consideration of all 3D planes, including axial, coronal and sagittal views in more cases are suggested in further studies to achieve more accurate and consistent results. Finally, 3D printed models are considered valuable tools in clinical practice, however, the time and cost associated with model generation and printing remain another limitation which needs to be addressed with technological improvements in 3D printers and cost reduction in printing materials as well as availability of automatic segmentation algorithms.

In conclusion, we have successfully generated a patient-specific 3D printed model of biliary system with congenital cyst. The 3D printed biliary model replicates anatomical structures of the biliary tract and the cyst with high dimensional accuracy in measurements of the cyst among these three different approaches. However, the large differences in anatomical measurements at different stages of the model production warrant further investigation. Future research is also needed to determine the clinical value of 3D printed biliary models in pre-surgical planning and simulation.

## Acknowledgements

None.

## Footnote

*Conflict of Interest:* The authors have no conflicts of interest to declare.

*Ethical Statement:* Ethical approval was obtained from Curtin University Human Research Ethics Committee (HRE20-18-0147). Informed consent was waived due to retrospective nature of the study and use of de-identified images.

## References

1. Giannopoulos AA, Steigner ML, George E Barile M, Hunsaker AR, Rybicki FJ, Mitsouras D. Cardiothoracic applications of 3-dimensional printing. *J Thorac Imaging*

- 2016;31:253-72.
2. Sun Z, Liu D. A systematic review of clinical value of three-dimensional printing in renal disease. *Quant Imaging Med Surg* 2018;8:311-25.
  3. Lau I, Sun Z. Three-dimensional printing in congenital heart disease: A systematic review. *J Med Radiat Sci* 2018;65:226-36.
  4. Tumbleston JR, Shirvanyants D, Ermoshkin N, Januszewicz R, Johnson AR, Kelly D, Chen K, Pinschmidt R, Rolland JP, Ermoshkin A, Samulski ET, DeSimone JM. Additive manufacturing: continuous liquid interface production of 3D objects. *Science* 2015;347:1349-52.
  5. Valverde I, Gomez-Ciriza G, Hussain T, Suarez-Mejias C, Velasco-Forte MN, Byrne N, Ordoñez A, Gonzalez-Calle A, Anderson D, Hazekamp MG, Roest AAW, Rivas-Gonzalez J, Uribe S, El-Rassi I, Simpson J, Miller O, Ruiz E, Zabala I, Mendez A, Manso B, Gallego P, Prada F, Cantinotti M, Ait-Ali L, Merino C, Parry A, Poirier N, Greil G, Razavi R, Gomez-Cia T, Hosseinpour AR. Three dimensional printed models for surgical planning of complex congenital heart defects: an international multicenter study. *Eur J Cardiothorac Surg* 2017;52:1139-48.
  6. Lim KH, Loo ZY, Goldie S, Adams J, McMenamin P. Use of 3D printed models in medical education: A randomized control trial comparing 3D prints versus cadaveric materials for learning external cardiac anatomy. *Anat Sci Educ* 2016;9:213-21.
  7. Costello JP, Olivieri L, Krieger A, Thabit O, Marshall MB, Yoo SJ, Kim PC, Jonas RA, Nath DS. Utilizing three-dimensional printing technology to assess the feasibility of high-fidelity synthetic ventricular septal defect models for simulation in medical education. *World J Pediatr Congenit Heart Surg* 2014;5:421-6.
  8. Costello JP, Olivieri LJ, Su L, Krieger A, Alfares F, Thabit O, Marshall MB, Yoo SJ, Kim PC, Jonas RA, Nath DS. Incorporating three-dimensional printing into a simulation-based congenital heart disease and critical care training curriculum for resident physicians. *Congenit Heart Dis* 2015;10:185-90.
  9. Lau I, Squelch A, Wan YL, Wong A, Ducke W, Sun Z. Patient-specific 3D printed model in delineating brain glioma and surrounding structures in a pediatric patient. *Digit Med* 2017;3:86-92.
  10. Aldosari S, Jansen S, Sun Z. Optimization of computed tomography pulmonary angiography using 3D printed model with simulation of pulmonary embolism. *Quant Imaging Med Surg* 2011;99:53-62.
  11. Ho D, Squelch A, Sun Z. Modeling of aortic aneurysm and aortic dissection through 3D printing. *J Med Radiat Sci* 2017;64:10-17.
  12. Kappanayil M, Koneti NR, Kannan RR, Kottavil BP, Kumar K. Three-dimensional-printed cardiac prototypes aid surgical decision-making and preoperative planning in selected cases of complex congenital heart diseases: early experience and proof of concept in a resource-limited environment. *Ann Pediatr Cardiol* 2017;10:117-25.
  13. Salmi M, Paloheimo KS, Tuomi J, Wolff J, Mäkitie A. Accuracy of medical models made by additive manufacturing (rapid manufacturing). *J Craniomaxillofac Surg* 2013;41:603-9.
  14. Waran V, Pancharatnam D, Thambinayagam HC, Raman R, Rathinam AK, Balakrishnan YK, Tung TS, Rahman ZA. The utilization of cranial models created using rapid prototyping techniques in the development of models for navigation training. *J Neurol Surg A Cent Eur Neurosurg* 2014;75:12-5.
  15. Lau IW, Liu D, Xu L, Fan Z, Sun Z. Clinical value of patient-specific three-dimensional printing of congenital heart disease: Quantitative and qualitative assessments. *PLoS One* 2018;13:e0194333.
  16. Baimakhanov Z, Soyama A, Takatsuki M, Hidaka M, Hirayama T, Kinoshita A, Natsuda K, Kuroki T, Eguchi S. Preoperative simulation with a 3-dimensional printed solid model for one-stop reconstruction of multiple hepatic veins during living donor liver transplantation. *Liver Transpl* 2015;21:266-8.
  17. Perica E, Sun Z. Patient-specific three-dimensional printing for pre-surgical planning in hepatocellular carcinoma treatment. *Quant Imaging Med Surg* 2017;7:668-77.
  18. Soejima Y, Taguchi T, Sugimoto M, Hayashida M, Yoshizumi T, Ikegami T, Uchiyama H, Shirabe K, Maehara Y. Three-dimensional printing and biotexture modeling for preoperative simulation in living donor liver transplantation for small infants. *Liver Transpl* 2016;22:1610-4.
  19. Zein NN, Hanouneh IA, Bishop PD, Samaan M, Eghtesad B, Quintini C, Miller C, Yerian L, Klatter R. Three-dimensional print of a liver for preoperative planning in living donor liver transplantation. *Liver Transpl* 2013;19:1304-10.
  20. Witowski J, Wake N, Grochowska A, Sun Z, Budzynski A, Major P, Popiela TJ, Pedziwiatr M. Investigating accuracy of 3D printed liver models with computed tomography. *Quant Imaging Med Surg* 2019;9:43-52.
  21. Perica ER, Sun Z. A systematic review of three-

- dimensional printing in liver disease. *J Digit Imaging* 2018;31:692-701.
22. Javan R, Zeman M. A prototype educational model for hepatobiliary interventions: unveiling the role of graphic designers in medical 3D printing. *J Digit Imaging* 2018;31:133-43.
  23. Javan R, Herrin D, Tangestanipoor A. Understanding spatially complex segmental and branch anatomy using 3D printing: liver, lung, prostate, coronary arteries, and circle of willis. *Acad Radiol* 2016;23:1183-9.
  24. Souzaki R, Kinoshita Y, Ieiri S, Hayashida M, Koga Y, Shirabe K, Hara T, Maehara Y, Hashizume M, Taguchi T. Three-dimensional liver model based on preoperative CT images as a tool to assist in surgical planning for hepatoblastoma in a child. *Pediatr Surg Int* 2015;31:593-6.
  25. Blender. Blender Foundation. Available online: <https://www.blender.org/foundation/>
  26. Takagi K, Nanashima A, Abo T, Arai J, Matsuo N, Fukuda T, Nagayasu T. Three-dimensional printing model of liver for operative simulation in perihilar cholangiocarcinoma. *Hepatogastroenterology* 2014;61:2315-6.
  27. Dhir V, Itoi T, Fockers P, Perez-Miranda M, Khashab MA, Seo DW, Yang AM, Lawrence KY, Maydeo A. Novel ex vivo model for hands-on-teaching of and training in EUS-guided biliary drainage: creation of "Mumbai EUS" stereolithography/3D printing bile duct prototype (with videos). *Gastrointest Endosc* 2015;81:440-6.

**Cite this article as:** Allan A, Kealley C, Squelch A, Wong YH, Yeong CH, Sun Z. Patient-specific 3D printed model of biliary ducts with congenital cyst. *Quant Imaging Med Surg* 2019;9(1):86-93. doi: 10.21037/qims.2018.12.01